ISSN 1341-562X

JOURNAL OF FOREST PLANNING

Vol. 21 No. 1
April, 2016

Japan Society of Forest Planning

JOURNAL OF FOREST PLANNING

Submission of Manuscripts

Manuscripts should be submitted to following Editorial Office.

Dr. Keiko NAGASHIMA
JOURNAL OF FOREST PLANNING
Graduate School of Life and Environmental Science, Kyoto Prefectural University
1-5, Hangi-cho, Shimogamo, Sakyo-ku, Kyoto 606-8522, Japan
Phone: +81-75-703-5635, Fax: +81-75-703-5635
E-mail: jsfp_e@forestplanning.jp

Notice about Photocopying

Subscription Information

JOURNAL OF FOREST PLANNING is published half yearly. The subscription for 2014 is 5,000 yen and the single issue price is 2,500 yen. Subscription orders can be sent to following office.

JOURNAL OF FOREST PLANNING is published by
Japan Society of Forest Planning
Graduate School of Life and Environmental Science, Kyoto Prefectural University
1-5, Hangi-cho, Shimogamo, Sakyo-ku, Kyoto 606-8522, Japan

JOURNAL OF

FOREST PLANNING

Vol.21, No.1 April, 2016

Japan Society of Forest Planning

CONTENTS

Articles

Article

Evaluation of Three-Dimensional Leaf Distribution within a Closed Canopy Based on Low-Cost Laser Scanning Data during Leafless Season

Takaharu Mochizuki[*1] and Hiromi Mizunaga[*2]

ABSTRACT

Foliage estimation from laser scanning data has limitations caused by the occluded space of beams in a canopy and high cost of the scanning. We focused on twigs supporting leaves, and developed an estimation method for three-dimensional foliage distribution with low-cost laser scanning under leafless conditions. To validate the scanning method, we used the method for the canopy of a secondary *Fagus crenata* forest and applied a contact point quadrat method to the canopy. Vertical leaf distribution from scanning during leafless season was very similar to that of the contact method, and the three-dimensional leaf distribution from the scanning showed a smooth trend of leaf area density within a canopy volume of $1.8 \times 1.8 \times 0.6$ m^3. These results were caused by the smaller proportion of occluded space and substantial reduction of estimation error per beam length. We can reduce the cost of our scanning system because of its minimal requirements. The concept of scanning during leafless season might have the potential to contribute to scanning with a high-resolution scanner by complementing the occluded space in an existing foliage estimation method using our estimation method.

keyword: forest canopy, terrestrial laser scanner, three-dimensional leaf distribution, low cost

INTRODUCTION

Foliage distribution is an important aspect of stand structure in ecological function by affecting stand microclimate, such as CO_2 flux (Wang and Jarvis, 1990; Sinoquet et al. 2001; Iio et al., 2011), stem shape (Oohata and Shinozaki, 1979; Chiba et al., 1988; Osawa, 1990), and resistance to wind damage (Zhu et al., 2001; Kitagawa et al., 2015). Many studies on foliage distribution have focused on vertical information (Monsi and Saeki, 1953; Pulkkinen, 1991; Maguire and Bennett, 1996), but did not treat the discontinuity of that distribution, which in theory modifies microclimate in the canopy through light transmittance (Kira et al., 1969; Castro and Fetcher, 1999). In the last three decades, the three-dimensional foliage distribution within forest canopies has been regarded as useful or crucial for forest structure and has been addressed in several research works (Kurachi et al., 1986; Koike, 1989; Morales et al., 1996; Fukushima et al., 1998; Sinoquet and Rivet, 1997; Mizunaga and Umeki, 2001; Iio et al., 2011; Mizunaga and Fujii, 2013). However, difficulties of accessing canopies have caused a scarcity of information on three-dimensional foliage distribution at canopy scale (Mizunaga and Fujii, 2013; Béland et al., 2014).

LiDAR (Light Detection And Ranging) (a list of abbreviations is available in Appendix) scanners have advantages in measuring three-dimensional locations and shapes of objects rapidly, precisely and nondestructively (Dassot et al., 2011). Terrestrial LiDAR scanners (TLS) have thus been used to measure volume and morphology of tree stems and branches in forests (Dassot et al., 2012; Dominik et al., 2013; Hosoi et al., 2013). However, estimation of the foliage distribution within forest canopies remains limited (Dassot et al., 2011; Seidel et al., 2011).

Foliage clusters with very dense foliage obstruct laser beams from detecting material behind them and prevent foliage estimation in the occluded space. This space is not sampled by a sufficient number of laser beams for reliable calculation of leaf area (Hosoi and Omasa, 2007; Takeda et al., 2008; Côté et al., 2009; Béland et al., 2011; Dassot et al., 2011; Béland et al., 2014). When applying TLS methods to a closed canopy, there is large estimation error of leaf area in the middle to upper layers of the canopy, because foliage in the lower layer intercepts numerous laser beams and reduces the number of incident laser beams in the middle and upper layers (Hosoi and Omasa, 2007). Coupling of airborne and

Corresponding author: Hiromi Mizunaga

[*1] The United Graduate School of Agricultural Science, Gifu University, Gifu 501-1193, Japan
[*2] Faculty of Agriculture, Shizuoka University, Suruga-ku, Shizuoka 422-8529, Japan
E-mail: mizunaga.hiromi@shizuoka.ac.jp (H. Mizunaga)

terrestrial scanning has been done to reduce the occluded space in a canopy (Hosoi et al., 2010), but space remained in its middle layer. Hosoi and Omasa (2007) suggested that scanning from a lateral viewpoint of a canopy decreased the amount of obstruction by shallow angled leaves there. However, lateral scanning requires heavy and expensive equipment such as lifts and towers for placing a TLS at high aboveground positions.

Although the cost of high-resolution TLS instruments has recently decreased (Dassot et al., 2011), it was still great. Furthermore, processing large amounts of LiDAR data is time-consuming and requires powerful computer hardware (Seidel et al., 2011). Such high costs of methods using LiDAR data limit the widespread use of TLS.

The foliage distribution is closely related to the distribution of stems and branches, which is the physical supporting system. The well-known relationship of pipe model theory is that a cross-sectional area of sapwood in stems (or branches) at a given point is proportional to the leaf amount attached to stems (or branches) above that point (Shinozaki et al., 1964a; Oohata and Shinozaki, 1979). This model suggests that younger stems (or branches) that are assumed to be composed of only new pipes have a closer relationship between their cross-sectional area and leaf amount than do older ones (Shinozaki et al., 1964b; Chiba, 1991; Turner et al., 2000; Sumida et al., 2009). Kakubari (1987) found a strong linear relationship between twig and leaf mass within a *Fagus crenata* canopy. Such a strong quantitative relationship between leaves and twigs permits estimation of foliage distribution via twig distribution. Côté et al. (2009) established virtual tree plants using the pipe model and TLS data for parts of conifer trees "visible" to TLS. Although their objective was to reconstruct virtual tree structure, the idea of linking TLS data and the pipe model connecting branches and leaves could be useful for measuring actual foliage distributions. We conceived the scanning of twigs during leafless season to estimate the three-dimensional leaf distribution.

Our objectives were to develop an estimate for three-dimensional foliage distribution with low-cost laser scanning during leafless season, and to validate this with full assessment of the three-dimensional leaf distribution in a canopy by direct measurement. The advantages of our foliage estimation technique were to: 1) acquire LiDAR data only from the ground; 2) avoid high-resolution, expensive TLS and perform low-cost scanning; 3) estimate foliage distribution in a closed-canopy forest and for an isolated canopy, and 4) develop the potential for complementing occluded space within a canopy in an existing foliage estimation method using TLS.

MATERIALS AND METHODS

Study site

The study stand was an approximately 80-year-old, secondary *Fagus crenata* forest at 900 m a.s.l. on the northeastern slope of Mount Naeba in Japan (36°55′ N, 138° 46′ E). Bedrock at the stand is predominantly tuff and augite-hypersthene acid andesite (Echigo-Yuzawa quadrangle series 1:50,000; Geological Survey of Japan, AIST, 1978), on which moderately moist brown forest soil has formed. During the period 1979−2012, mean annual precipitation and temperature at a nearby Yuzawa meteorological station (36° 56′ N, 138°49′ E, 340 m a.s.l.; Japanese Bureau of Meteorology) were 2,224 mm and 11.5℃, respectively. Around 3−4 m of snow accumulates at the stand during December through March. Mean tree height, mean diameter at breast height of the trunks (1.3 m), and tree density were respectively 18.8 m, 24.7 cm and 950 trees ha^{-1} in a 20 m × 30 m plot established in the stand. Basal area of *Fagus crenata* was 96% of total basal area of the plot. Beginning of leaf flush and end of leaf fall within the *Fagus crenata* canopy of the plot were in late April and mid November, respectively. Further details about the plot are in Iio et al. (2005) and Kubota et al. (2005).

A 26.0-m tall canopy access tower was established above a 5.4 m × 5.4 m area of the plot (Fig. 1). The tower surrounded the entire crown of a dominant tree (tree height (H_t) = 23.5 m, lowest foliage height (H_l) = 14.2 m, *Fagus crenata*), a suppressed tree (H_t = 18.0 m, H_l = 5.0 m, *Fagus crenata*), and a part of crown of dominant trees (H_t = 23.0 m, H_l =7.4 m, *Fagus crenata*; H_t = 24.0 m, H_l =12.9 m, *Fagus crenata*).

Description of inexpensive scanner with combination of a range finder and rotation stage

We used a combination of a laser range finder (LDM 301.110, Jenoptik AG, Jena, Germany) and a rotation stage (PTU-D46-70, Directed Perception Inc., Burlingame, CA, USA) controlled by a PC according to Takeda et al. (2008) as an inexpensive scanner system. The laser range finder emitted rectangular laser beams with measurement range 0.5−300 m. Full scanning range of the inexpensive system was 0 to 2π rad azimuth angle and 0 to 1.4 rad zenith angle. In comparison with an expensive scanning system, the FARO Focus 3D 120 (FARO, Lake Mary, FL, USA), which has high-resolution and usable in forests (Dassot et al., 2011), acquisition speed of the inexpensive system was 63 points s^{-1} and 1/15,000 that of the expensive system. That is, the angular resolution of the inexpensive system was 1/120 that of the latter expensive system, with the same angular range and measurement time. The inexpensive system had laser spot size 40 mm × 9 mm upon leaving the instrument, and laser divergence angle 0.08 mrad × 1.7 mrad. It therefore had a laser spot area at distance 15 m from the instrument of 1420 mm^2 (41 mm × 34 mm), 47 times that of the expensive system, resulting in coarser resolution.

We scanned the canopy of *Fagus crenata* stand in an 11.4 m × 15 m plot (Fig. 1) using the system, during 4−5 August 2010 (leafy season) and five windless days (17−24 November 2011, leafless season). The zenith angle for scanning was 0 to 0.9 rad at 7-mrad interval. Azimuth angle range was point-specific (Fig. 1), with 3.5 mrad interval in both seasons (this is called coarser scanning hereafter). In addition to the coarser scanning, we scanned the canopy with zenith angle range 0 to 0.5 rad at 7 mrad interval, and azimuth angle at 1.7 mrad interval (finer scanning) during the leafless season particularly to focus the upper layer of the canopy where a shortage of the number of laser beams tend to occur. Each scan was conducted from 12 emission points (Fig. 1). We cleared shrubs and understory vegetation by pulling with ropes, to maintain visibility from the emission point. We determined the coordinate of that point by a total station (GPT-1004F, Topcon Positioning Systems Inc., Tokyo, Japan), in order to transform the scanning data into a common geometric coordinate system. We took hemispherical photographs using a digital camera (D60, Nikon, Tokyo, Japan) and fisheye lens (4.5mm F2.8 EX DC Circular Fisheye HSM, Sigma, Kanagawa, Japan) at the emitting points for acquiring color image of woody organs in the field of view of the scanning system with explicit directions of the pixels.

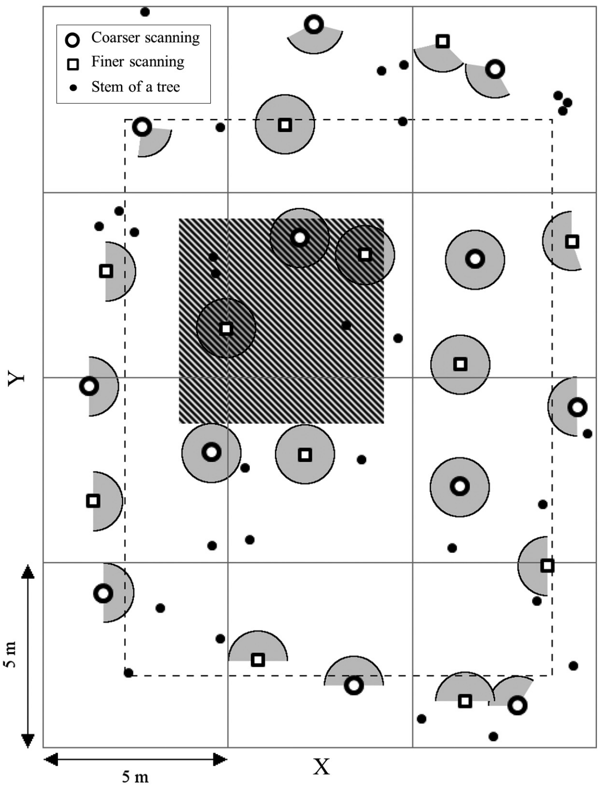

Fig. 1 Map of emission points of laser scanner. Area enclosed by dotted line is analysis range of scanning method (11.4 m × 15 m). Shaded area is an area surrounded by a canopy access tower and analysis range of contact point quadrat method (5.4 m × 5.4 m), respectively. Arcs and circles centered emitting points represent azimuth angle range of scanning.

Relationships between twig biometric measures and leaf area

We defined twigs as woody organs within 50 cm of tips of a branch. We sampled 29 shoots having main axis lengths 0.4−0.6 m (Fig. 2A) randomly located throughout the canopy in August or September 2010, to determine the relationship between twig biometric measures and leaf area. No sample shoot had a current year shoot with length > 50 cm. Two biometric measures of the sampled shoots were obtained as 1) the projection area of a twig from right angle to adaxial surface, and 2) the sum of inter-node length within a shoot (SIL hereafter) (Fig. 2B). Leaf area attached to the shoot was measured by a flatbed scanner and LIA32 software (Yamamoto, 2003).

The projection area of a twig may be suitable for estimating leaf area. However, estimating the projection area using our inexpensive scanning system had a difficulty owing to its beam size. Diameter of a laser beam in our system was > 34 mm in a canopy at a distance of 15 m from the emission point, and more than four times the twig base diameter, but the system was able to detect parts of a twig covering cross section area of the beam over 3%. It means that the beam detects the existence of twigs regardless branch diameter. In this case, it was impossible to determine the diameter at each portion of a twig, and scan data would fail to determine projection area with overestimation (Fig. 2C). The sum of area of laser beams which is intercepted by a twig should be proportional to the sum of inter-node length. Thus, we chose SIL as a representative biometric measure of a twig for feasible access using the scanning system with large beam diameter, after examining the relationships between SIL, projection area of a twig, and leaf area attached to a twig:

$$LA_s = b \times SIL_s^{\ c}, \tag{1}$$

where LA_s and SIL_s are leaf area attached to a shoot (m^2) and SIL within the shoot (m). b and c are a coefficient and a scaling exponent of the power trend line.

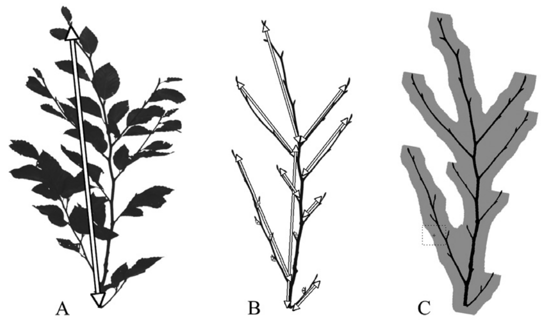

Fig. 2 Explanation of twig biometric measures. (A) A sampled shoot. A white arrow indicates main axis length. (B) A sampled twig. White arrows indicate inter-node length, and the sum of white arrow length is the sum of inter-node length within a shoot (SIL). (C) Laser beam interception of a twig. Dotted line and cross indicate a laser spot size (41 mm × 34 mm) at distance 15 m and center of the laser spot, respectively. Black and gray parts indicate a projection of a twig and area of laser beams intercepted by a twig, respectively.

Direct measurement of leaf area density

A contact point quadrat method (Wilson,1959) is a direct and non-destructive method for measuring foliage distribution and was applied to estimating three-dimensional foliage distribution within a forest canopy by Iio et al. (2011). We used the method to determine leaf area density (LAD) in a cuboidal cell (termed voxel) with volume 0.3 m × 0.3 m × 0.2

m within the access tower (Fig. 1), to validate LAD estimated by laser scanning. The measurement was conducted on eight days during early August 2011 by eight people. We penetrated a fine rod of 5-mm diameter into the voxel six times and counted the number of leaves contacting the rod. We measured the contacted leaf number of 28,188 voxels at 7.4−24.8 m above ground surrounded by the access tower (5.4 m × 5.4 m). The contacted leaf number was assumed to be 0.5 when no leaf contacted the rod, even though some leaves were visually observed in the voxel (Iio et al. 2011). We regressed the contacted leaf number data with LAD, which was obtained from a destructive method in 41 voxels distributed randomly in the entire canopy. Further details about the procedure of the method is in Iio et al. (2011).

We randomly set five circular litter traps with 0.25 m^2 projected area under the canopy in the 20 m × 30 m plot surrounding the plot of the contact point quadrat method and scanning from August through November 2011, to estimate leaf area index (LAI) in the canopy.

Estimation of LAD using scanning data during leafless season

We estimated LAD using the scanning data from leafless season in three steps: (1) Classification of twigs and other woody organs (stems and branches) from the scanning data; (2) computation of the SIL distribution within the canopy, (3) calculation of LAD using the SIL distribution and equation for the relationship between SIL and leaf area in a shoot.

We reconstructed a hemispherical image based on distance data of obstructive clouds from each emission point during leafless season, to extract the point cloud of twigs (Fig. 3). We removed point clouds longer than 50 cm from tips of branches by manually selecting the point cloud in the hemispherical image, referring to an actual hemispherical photograph. The filtering procedure required 1−1.5 hours for each scan. All filtered scans were transformed into a common geometric coordinate system using coordinates of the emission points.

We estimated SIL distribution with modifying PAD (Plant area density) estimation method by Béland et al. (2011). Béland et al. (2011) applied a contact point quadrat method (Wilson, 1959) to LiDAR scanning data and estimated PAD in a voxel, using a number of intercepts per unit length of laser beams (IF) from Eqs. (2) and (3).

$$IF = \frac{N_i}{l}, \tag{2}$$

where l and N_i are total length of a track of laser beams inside a voxel (m) and the number of beams intercepted by obstacles in the voxel, respectively.

$$PAD_v = \frac{IF}{G(\theta)}, \tag{3}$$

where PAD_v, $G(\theta)$ and IF are PAD in a voxel (m^2 m^{-3}), projected area of a unit foliage area on a plane perpendicular to a given laser incident zenith angle θ (rad), and projected area of obstacles intercepting laser beams per unit volume in a voxel (m^2 m^{-3}), respectively. Denoting α that mean length of

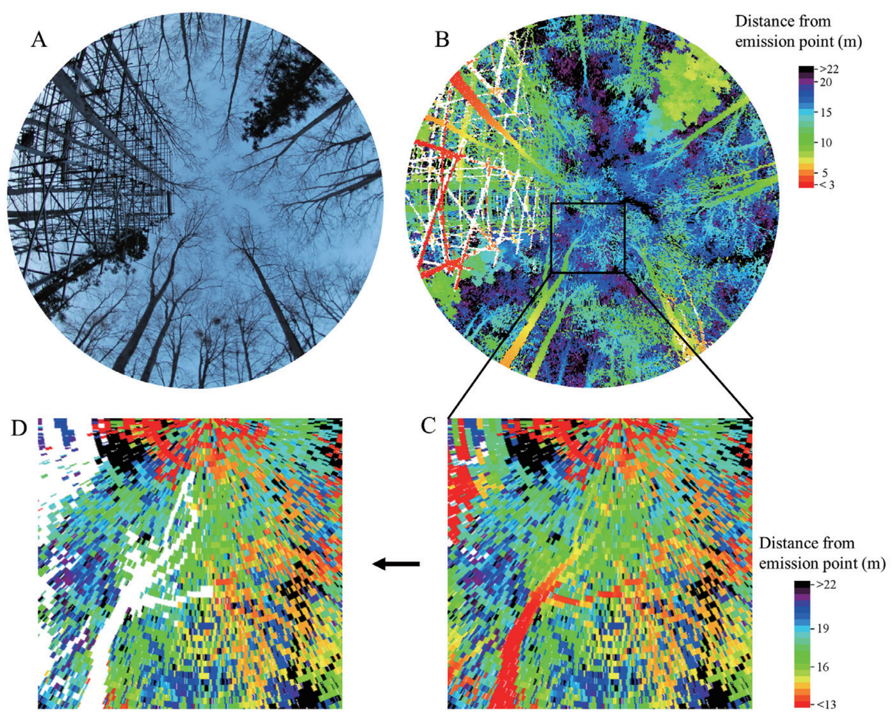

Fig. 3 Extracted point clouds of twigs in scanning data. (A) Hemispherical photograph taken at the emission point of laser scanner. (B) Hemispherical image constructed from scanning data. (C) Enlarged image of scanning data. (D) Image of scanning data after filtering procedure. White parts in images indicate lack of distance data, removed point clouds of woody organs (stems and branches) in filtering procedure, or point clouds of objects outside the analysis (canopy access tower).

a segment transecting a cross section of the beam per unit area of the cross section (m m^{-2}), SIL can be calculated by multiply of α. We used a spherical angular distribution for leaf angle, and then the $G(\theta)$ should be 0.5.

$$SIL_v = \frac{\alpha \cdot IF}{0.5}, \quad (4)$$

where SIL_v is SIL per unit volume in a voxel (m m^{-3}). Size of the probe is constant in the contact point quadrat method, but it varies with distance from the emission point in the scanning method. The correction value of α indicates a coefficient for beam size variation.

We calculated LAD in a voxel with 0.6 × 0.6 × 0.6 m^3 volume from the scanning data during leafless season within the canopy of the scanning plot. Substituting SIL_v for SIL_s in Eq. (1) gives the LAD of a voxel.

Data analyses

Criteria of length of incident beams in a voxel

Bråthen and Hagberg (2004) related LAD estimation error by the number of probes or penetrated probe length in plant communities. We determined the relationship between total probe length in a voxel and root-mean-square error (RMSE) of LAD through a resampling method for the voxels, in which total probe length exceeded 640 m as follows. We resampled incident laser beams in the voxel by randomly omitting beams to make total probe length approximately 320, 160, 80, 40, 20 and 10 m in the voxel, and calculated LAD in each total probe length class. Resampling procedures were repeated 10,000 times, and the calculated RMSE of LAD was based on the original LAD in each voxel and probe length class.

Validation estimated LAD using scanning method

We calculated a moving average of LAD using the scanning method and that measured by the contact point quadrat method, with horizontal side length class 0.6–3.0 m and 0.6 m intervals in each voxel.

Statistical analyses

We executed generalized linear mixed-effects models (GLMMs) for leaf area attached to a shoot and projection area of a twig as the response variable logarithmic SIL as a fixed effect, and sample trees as a random effect with Gaussian error distribution and a log link function. We established a generalized linear model (GLM) for the RMSE of estimated LAD from resampled data in voxels with LAD > 0.5 m^2 m^{-3} as the response variable total probe length as a fixed effect, with a Gaussian error distribution and log link function. We established GLM for total probe length in a voxel > 40 m and 80 m as the response variable height from the ground and scanning methods as fixed effects, with a binomial error

Table 1 Test for effects of sum of internode length within a shoot (SIL_s) on leaf area attached to the shoot and projection area of the twig in the shoot, using generalized linear mixed-effects model

Response variables	Fixed-effect factors	Estimate	Standard error	*T* value	*p*
Leaf area attached to a shoot (m^2)	Intercept	−2.37	0.18	−13.0	<0.001
	log$_e$ SIL_s (m)	0.63	0.1	6.39	<0.001
Projection area of a twig (m^2)	Intercept	−5.84	0.15	−37.8	<0.001
	log$_e$ SIL_s (m)	1.1	0.1	11	<0.001

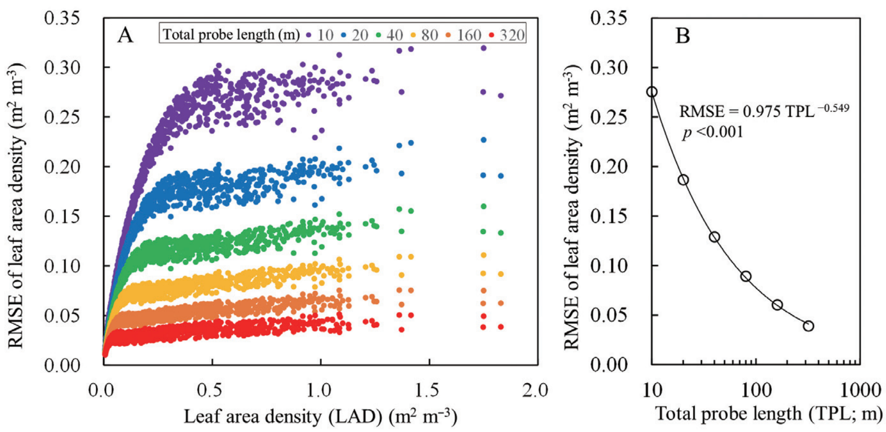

Fig. 4 (A) Effects of total probe length and LAD in a voxel on root-mean-square error (RMSE) of estimated LAD from resampled data. Each point indicates one voxel. (B) Effects of total probe length on RMSE of estimated LAD. RMSE was calculated based on voxels with LAD > 0.5 m^2 m^{-3}. Solid line indicates predicted values from GLM.

distribution and a logit link function. We assumed a linear relationship without an intercept between LAD estimated via the scanning method and that measured by the contact point quadrat method, and examined the difference between the slope of the linear model and a slope of 1 by t-test. All statistical analyses were conducted using R statistical software version 3.1.2 (R Core Team, 2014), including the lme 4 package (Bates et al., 2015).

RESULTS

Table 1 shows the allometric relationship of leaf area and projection area of twigs in shoots versus SIL. Scaling exponents of the power function obtained from the GLMM were 0.63 and 1.10 for leaf area and projection area of twigs, respectively.

The RMSE of the estimated LAD from resampled data versus estimated LAD from the parent set increased with LAD in a voxel asymptotically, in every total probe length class (Fig. 4A). The RMSE of LAD in voxels with LAD > 0.5 $m^2\ m^{-3}$ decreased exponentially with length (or resampling proportion) (Fig. 4B). The RMSEs at the asymptotic point were < 0.16 $m^2\ m^{-3}$ and < 0.11 $m^2\ m^{-3}$ for lengths 40 m and 80 m, respectively. The RMSE reached the asymptotic point at lower LAD for a longer total probe length.

The proportion of voxels with total probe length longer than 40 m and 80 m in the scanning data during leafy season decreased with height from the ground, especially for the base of the crown of *Fagus crenata* at 13 m above ground (Fig. 5A and B). This height was lower than that in leafless season (Table 2). The proportions for 40 m total probe length at the upper canopy at 22.4 m height (near the canopy top) were 4.8%, 45.1% and 84.4% in the coarser scanning during leafy season, coarser scanning during leafless season, and a combination of finer and coarser scanning during leafless season, respectively.

Vertical leaf distribution patterns scanned during leafless season including coarser and the finer and coarser combination were similar to that measured by the contact point quadrat method (Fig. 6). Conversely, that scanned during leafy season skewed downward compared to the other method, and had 1.5–2 times the leaf area at 15–20 m above ground. RMSE of scanned leaf area per 0.6 m horizontal layer based on measurement by the contact method was 5.60 in leafy season, five times that in leafless

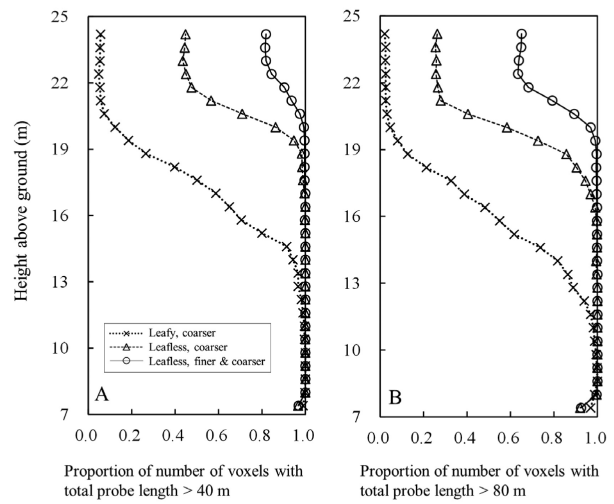

Fig. 5 Differences in vertical profile of total probe length in a voxel within the scanned canopy, between three scanning methods (coarser scanning in leafy season, coarser scanning in leafless season, and combination of finer and coarser scanning in leafless season).

Table 2 Test for effects of height of voxel from the ground and scanning methods, for total probe length in a voxel longer than 40 m and 80 m using generalized linear model

Response variables	Fixed effect factors	*Z*-value	*p*
Total probe length > 40 m	Intercept	74.3	<0.001
	Height above ground (m)	−75.3	<0.001
	Leafy, coarser	–	–
	Leafless, coarser	59.2	<0.001
	Leafless, finer and coarser	71.8	<0.001
Total probe length > 80 m	Intercept	83.4	<0.001
	Height above ground (m)	−85.7	<0.001
	Leafy, coarser	–	–
	Leafless, coarser	58.1	<0.001
	Leafless, finer and coarser	77.1	<0.001

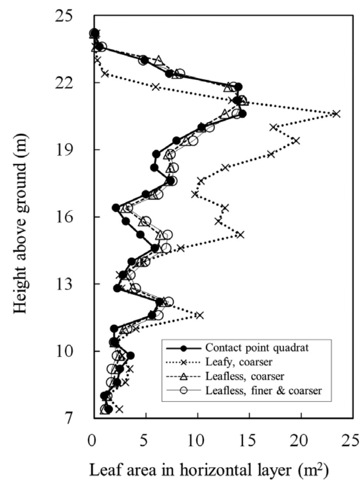

Fig. 6 Vertical leaf distribution patterns estimated using the scanning methods and contact point quadrat method. Leaf area was summed in each horizontal layer of thickness = 0.6 m above the plot (5.4 × 5.4 m^2), using the contact point quadrat method.

Table 3 Differences of leaf area per 0.6 m horizontal layer and leaf area index (LAI) between estimation methods

Estimation method	RMSE of leaf area (m^2)	LAI ($m^2\ m^{-2}$)
Coarser scanning in leafy season	5.6	8.28
Coarser scanning in leafless season	0.93	5.36
Finer and coarser scanning in leafless season	1.12	5.51
Contact point quadrat method	–	5.06
Litter–trap method	–	5.74

Root-mean-square error (RMSE) of leaf area from scanning methods was based on leaf area measured by contact point quadrat method.

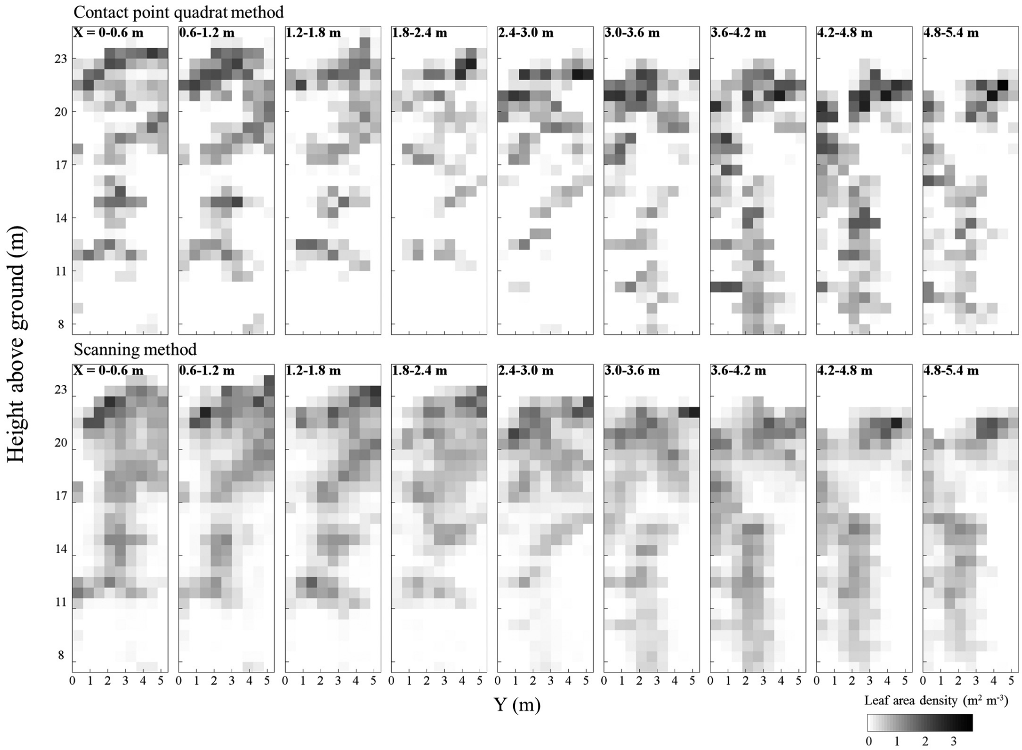

Fig. 7 Visualization of LAD distribution measured by contact point quadrat method and that estimated from scanning data in leafless season. Thickness of the vertical section is 0.6 m. The x-axis coordinate is shown in upper left-hand corner of each graph.

season. The large error in leafy season caused overestimation of LAI, whereas LAI estimated by scanning during leafless season almost equaled that from the contact point quadrat and litter trap methods (Table 3).

Although the vertical leaf distribution from scanning in leafless season corresponded to that measured by the contact point quadrat method, a vertical section of three-dimensional distribution shows a different pattern between scanned and measured (Fig. 7). Images from the scanning show similar trends as the contact point quadrat method but they were blurry, with more voxels showing moderate LAD values.

Scanned LAD had a determination coefficient against measured LAD of 0.65 (Table 4) and overestimated by less than 1.0 m^2 m^{-3} the measured LAD, but underestimated by greater than 1.5 m^2 m^{-3} the measured LAD in a single voxel based calculation (no moving average) (Fig. 8). However, the estimation was improved by a moving average along the horizontal direction with increasing determination coefficient, decreasing RMSE, and slope near 1.0 (Table 4). There was no clear bias from the 1:1 line when averaged voxel number was > 16. A moving average of nine voxels gave a determination coefficient of 0.87 and RMSE of 0.17, with a regression slope of 0.93 between scanned and measured LAD.

DISCUSSION

The asymptotically increasing RMSE of resampled LAD with increase of original LAD (Fig. 4A) implies that relative estimation error decreased with a larger original LAD. Bråthen and Hagberg (2004) showed a minor effect of leaf biomass in plant communities on relative estimation error in the contact point quadrat method. Their result contradicts our finding. Because accuracy based on a unit of contact (or intercept beam) is constant, the relative estimation error derived from that accuracy is larger with lower contact frequency, owing to the inversely proportional relationship. The large relative estimation error for small LAD could not be ignored in our study, because the intercept frequency of beams by twigs in our method was expected to be lower than direct contact frequency of leaves with larger projected area.

The RMSE of LAD decreased exponentially with greater probe length, concurring with the result of Hosoi and Omasa (2007). They believed that reduction of the scaling exponent demonstrated improved accuracy with probe number or length, and they found that exponents in the relationship increased from -0.48 to -0.26 as the angle between beam and leaf surface increased (i.e., a larger projected area from the beam direction). They concluded that a smaller projection area from the beam direction increased transmitted beams and gave a greater reduction in estimation error with probe number. As a result of the small projected area of twigs, the scaling exponent of -0.55 in our method (Fig. 4B) was smaller than that of Hosoi and Omasa (2007).

The proportions of voxels with total probe length shorter than 40 m and 80 m in leafy season increased at > 13 m from the ground (Fig. 5), and were > 93% and 97% above 20 m from the ground, respectively. The proportions during leafy season reveal the difficulty of measuring LAD of the upper crown in leafy season, because of a large proportion of occluded space (Fig. 5). Proportions in leafless season were <

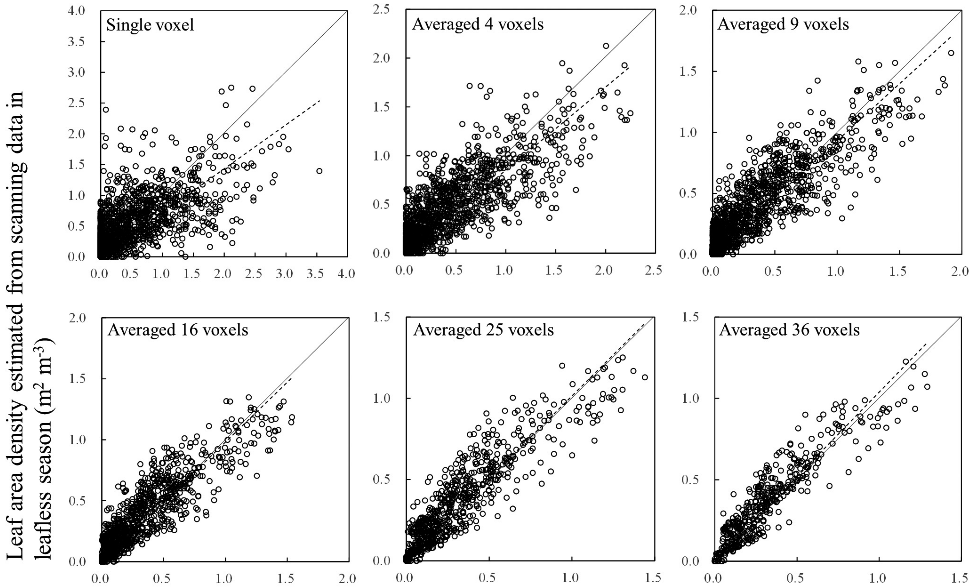

Fig. 8 Change of relationship between moving average of LAD estimated from the scanning data in leafless season and that measured by contact point quadrat method with sample range of the moving average. The number of voxels within the sample range of the moving average is shown in upper left-hand corner of each graph. Dashed and solid lines in each figure represent regression and 1:1 lines.

Table 4 Summary statistics for relationship between moving average of LAD estimated using scanning data in leafless season and that measured by contact point quadrat method

Number voxels in sample range of the moving average	Slope of regression line	Standard error	p-value of slope from slope = 1	Determination coefficient	RMSE (m^2 m^{-3})
1	0.72	0.011	<0.001	0.65	0.35
4	0.85	0.009	<0.001	0.82	0.23
9	0.93	0.01	<0.001	0.87	0.17
16	0.98	0.01	0.063	0.9	0.15
25	1.01	0.011	0.201	0.92	0.13
36	1.04	0.012	0.001	0.94	0.11

56% and 75% in the coarser scanning and < 19% and 37% with the combination of finer and coarser scanning 20 m above the ground, respectively. These results suggest that the scanning in leafless season improved the proportion of the explored voxel (Fig. 5). This result agrees with accurate measurement of stem and main branch structure by scanning during leafless season (Dassot et al., 2012; Dominik et al., 2013; Hosoi et al., 2013).

The difference of vertical leaf distribution patterns between scanning in leafy season and measurement by the contact point quadrat method was substantial at 15 m above the ground (Fig. 6). Estimation error may be caused by the decrease of total probe length caused by foliage obstruction in lower canopy layers, because the height of large error was similar to the height where the reduction of total probe length appeared (Fig. 5). This agrees with the result of Hosoi and Omasa (2007). The scanning in leafless season showed a very similar vertical LAD pattern to that of the contact point quadrat method, with small estimation error (Table 3). Moreover, LAI estimated from scanning in leafless season was similar to that measured by the contact point quadrat method and litter-trap data (Table 3). This result suggests that scanning (even just the coarse variety) in leafless season by an inexpensive system would permit a practical rough census of canopy structure and leaf biomass. Effective estimation of vertical leaf distribution was achieved by fewer occluded spaces and efficient reduction of estimation error per probe length during leafless season.

The blurry image of the vertical section in the scanned LAD map (Fig. 7) and estimation improved by a moving average using more than nine voxels suggest that scanning produced more moderate LAD values. For example, the relationship between estimated and measured LAD in a single voxel altered the pattern of LAD estimation error by 1.0 m^2 m^{-3}. That is, there was overestimation in voxels with LAD < 1.0 m^2 m^{-3} and underestimation in those with LAD > 1.0 m^2 m^{-3} (Fig. 8). Coefficients of variation of the scanned and measured LAD in a single voxel were 136% and 184%, respectively. Two possible factors causing the moderate LAD from scanning were noise in distance measurement from scanning, which is frequent near obstacle edges (Van der Zande et al., 2006; Cifuentes et al., 2014), and in the merger of data from emission points into a common geometric coordinate system. The influence of error determined by emission direction (leveling and initial azimuth error) increases with distance from the emission point, and can interfere with precise determination of the common coordinates of a point cloud. The above error factors possibly dispersed point clouds and homogenized point densities, with decreased concentration of point clouds.

The LAD values averaged using more than nine voxels in the scanning agreed with those from the contact point quadrat method (Fig. 8, Table 4). The volume of space for the averaged voxels was equivalent to $1.8 \times 1.8 \times 0.6$ m^3. The moving-average values eliminated variation of values within the data. This means that leaf clumping and noise less than the sample range of a moving average were filtered out. The result suggests that our scanning detected only leaf clusters larger than $1.8 \times 1.8 \times 0.6$ m^3, failing to detect smaller ones. However, the scanning could estimate smoothed trends of three-dimensional leaf distribution, for example LAD change from the crown edge to the center of each tree or the difference between individual trees. This smoothed trend helps establish a leaf distribution function composed of depth from the crown surface and distance from the crown center, like the foliage distribution model of Mizunaga and Umeki (2001).

The contact point quadrat method was effective for describing the three-dimensional distribution of LAD in forest canopies. However, this required equipment that limited application to forests with easy accessibility. An example is a tower, for direct access to canopies at high aboveground positions. Conversely, it is possible to apply our scanning method to various forests, owing to ground-based and non-destructive measurement and scanning system portability (weight of the system was < 15 kg). Labor-intensity of our scanning method was substantially lower than that of the contact point quadrat method; requiring two people for five working days for laser scanning and one operator for four working days for point cloud processing to cover a 3000 m^3 canopy volume, totally 14 person-days here, while the contact point quadrat method required eight people for eight working days, totally 64 person-days, for field measurements to cover a canopy volume of 500 m^3.

Since twigs in a shoot have a smaller surface area or projection area than a shoot with attached leaves, our method required the scanning system to sensitively detect twigs in the canopy. Our LAD estimation required a total number of beams ~3,800,000 in the 11.4 m × 15 m plot during leafless season. Because even the low-cost scanning system satisfied these requirements, we could reduce its cost to about JPY 1,000,000 in 2008.

Although our study aimed to develop low-cost scanning for leaf distribution, the concept of scanning during leafless season might have potential for use with a high-resolution scanner. Even using such a scanner, occluded space in a closed stand was still a major problem for LAD estimation (Hosoi and Omasa, 2007; Béland et al., 2011; Béland et al., 2014). Our estimation method using scanning data during leafless season overcame this problem of occluded spaces. We suggest scanning during both leafy and leafless season to complement occluded space in the existing foliage estimation method by our estimation method. Such a complementary approach will facilitate a census of canopy structure, including a closed-canopy forest, based on the three-dimensional LAD distribution. We currently use the method with high-resolution scanning during both leafy and leafless seasons for closed-canopy forests, and can adequately measure the three-dimensional LAD distribution in the canopy.

LITERATURE CITED

Bates, D., Maechler, M., Bolker, B. and Walker, S. (2015) lme4: Linear mixed-effects models using Eigen and S4. R package version 1.1-8. http://CRAN.R-project.org/package=lme4 (Accessed on 8 August 2015)

Béland, M., Widlowski, J. L., Fournier, R., Côté, J. F. and Verstraete, M. M. (2011) Estimating leaf area distribution in savanna trees from terrestrial LiDAR measurements. Agric. For. Meteorol. **151**: 1252-1266

Béland, M., Baldocchi, D. D., Widlowski, J. L., Fournier, R. A. and Verstraete, M. M. (2014) On seeing the wood from the leaves and the role of voxel size in determining leaf area distribution of forests with terrestrial LiDAR. Agric. For. Meteorol. **184**: 82-97

Bråthen, K. A. and Hagberg, O. (2004) More efficient estimation of plant biomass. J. Veg. Sci. **15**: 653-660

Cifuentes, R., Van der Zande, D., Salas, C., Farifteh, J. and Coppin, P. (2014) Correction of erroneous LiDAR measurements in artificial forest canopy experimental setups. Forests **5**: 1565-1583

Chiba, Y., Fujimori, T. and Kiyono, Y. (1988) Another interpretation of the profile diagram and its availability with consideration of the growth process of forest trees. J. Jpn. For. Soc. **70**: 245-254

Chiba, Y. (1991) Plant form based on the pipe model theory II. Quantitative analysis of ramification in morphology. Ecol. Res. **6**: 21-28

Côté, J. F., Widlowski, J. L., Fournier, R. A. and Verstraete, M. M. (2009) The structural and radiative consistency of three-dimensional tree reconstructions from terrestrial lidar. Remote. Sens. Environ. **113**: 1067-1081

Dassot, M., Constant, T. and Fournier, M. (2011) The use of terrestrial LiDAR technology in forest science: application fields, benefits and challenges. Ann. For. Sci. **68**: 959-974

Dassot, M., Colin, A., Santenoise, P., Fournier, M. and Constant, T. (2012) Terrestrial laser scanning for measuring the solid wood volume, including branches, of adult standing trees in the forest environment. Comput. Electron. Agric. **89**: 86-93

de Castro, F. and Fetcher, N. (1999) The effect of leaf clustering in the interception of light in vegetal canopies: theoretical considerations. Ecol. Model. **116**: 125-134

Bayer, D., Seifert, S. and Pretzsch, H. (2013) Structural crown properties of Norway spruce (*Picea abies* [L.] Karst.) and

European beech (*Fagus sylvatica* [L.]) in mixed versus pure stands revealed by terrestrial laser scanning. Trees **27**: 1035-1047

Fukushima, Y., Hiura, T. and Tanabe, S. (1998) Accuracy of the MacArthur-Horn method for estimating a foliage profile. Agric. For. Meteorol. **92**: 203-210

Iio, A., Fukasawa, H., Nose, Y., Kato, S. and Kakubari, Y. (2005) Vertical, horizontal and azimuthal variations in leaf photosynthetic characteristics within a *Fagus crenata* crown in relation to light acclimation. Tree physiol. **25**: 533-544

Iio, A., Kakubari, Y. and Mizunaga, H. (2011) A three-dimensional light transfer model based on the vertical point-quadrant method and Monte-Carlo simulation in a *Fagus crenata* forest canopy on Mount Naeba in Japan. Agric. For. Meteorol. **151**: 461-479

Hosoi, F. and Omasa, K. (2007) Factors contributing to accuracy in the estimation of the woody canopy leaf area density profile using 3D portable lidar imaging. J. Exp. Bot. **58**: 3463-3473

Hosoi, F., Nakai, Y. and Omasa, K. (2010) Estimation and error analysis of woody canopy leaf area density profiles using 3-D airborne and ground-based scanning Lidar remote-sensing techniques. IEEE Trans. Geosci. Remote Sens. **48**: 2215-2223

Hosoi, F., Nakai, Y. and Omasa, K. (2013) 3-D voxel-based solid modeling of a broad-leaved tree for accurate volume estimation using portable scanning lidar. ISPRS J. Photogramm. **82**: 41-48

Kakubari, Y. (1987) Modelling the productive structure and function of natural forests of *Fagus crenata* at different altitudes in Naeba Mountains. An analysis of dry matter production with an eco-physiological computer simulation model based on an individual tree. Bull. Tokyo Univ. For. **76**: 107-162

Kira, T., Shinozaki, K. and Hozumi, K. (1969) Structure of forest canopies as related to their primary productivity. Plant. Cell. Physiol. **10**: 129-142

Kitagawa, K., Iwama, S., Fukui, S., Sunaoka, Y., Yazawa, H., Usami, A., Naramoto, M., Uchida, T., Saito, S. and Mizunaga, H. (2015) Effects of components of the leaf area distribution on drag relations for *Cryptomeria japonica* and *Chamaecyparis obtusa*. Eur. J. For. Res. **134**: 403-414

Koike, F. (1989) Foliage-crown development and interaction in *Quercus gilva* and *Q. acuta*. J. Ecol. **77**: 92-111

Kubota, M., Tenhunen, J., Zimmermann, R., Schmidt, M., Adiku, S. and Kakubari, Y. (2005) Influences of environmental factors on the radial profile of sap flux density in Fagus crenata growing at different elevations in the Naeba Mountains, Japan. Tree Physiol. **25**: 545-556

Kurachi, N., Hagihara, A. and Hozumi, K. (1986) Distribution of leaf- and branch-biomass density within a crown of Japanese Larch and its relationship to primary production: Analysis by sainome-cutting. In: Fujimori, T. and Whitehead, D. (eds) Crown and canopy structure in relation to productivity. Forestry and Forest Products Research Institute, Ibaraki, Japan, 308pp

Maguire, D. A. and Bennett, W. S. (1996) Patterns in vertical distribution of foliage in young coastal Douglas-fir. Can. J. For. Res. **26**: 1991-2005

Mizunaga, H. and Umeki, T. (2001) The relationships between tree size and spatial distribution of foliage-mass within crowns of Japanese cedars (*Cryptomeria japonica*) in young plantations. For. Ecol. Manage. **149**: 129-140

Mizunaga, H. and Fujii, K. (2013) Is foliage within crowns of *Cryptomeria japonica* more heterogeneous and clumpy with age? J. Sustain. For. **32**: 266-285

Monsi, M. and Saeki, T. (1953) Über den lichtfaktor in den pflanzengesellschaften und seine bedeutung für die stoffproduktion. Jpn. J. Bot. **14**: 22-52

Morales, D., Jiménez, M. S., González-Rodríguez, A. M. and Cermák, J. (1996) Laurel forests in Tenerife, Canary Islands. II. Leaf distribution patterns in individual trees. Trees **11**: 41-46

Oohata, S. and Shinozaki, K. (1979) A statistical model of plant form−Further analysis of the pipe model theory. Jpn. J. Ecol. **29**: 323-335

Osawa, A. (1990) Reconstructed development of stem production and foliage mass and its vertical distribution in Japanese larch. Tree Physiol. **7**: 189-200

Pulkkinen, P. (1991) Crown structure and partitioning of aboveground biomass before the competition phase in a mixed stand of normal-crowned Norway spruce (*Picea abies* (L.) Karst.) and pendulous Norway spruce (*Picea abies* f. pendula (Lawson) Sylven). Tree Physiol. **8**: 361-370

R Core Team (2014) R: A language and environment for statistical computing. http://www.R-project.org/ (Accessed on 8 August 2015)

Seidel, D., Fleck, S., Leuschner, C. and Hammett, T. (2011) Review of ground-based methods to measure the distribution of biomass in forest canopies. Ann. For. Sci. **68**: 225-244

Shinozaki, K., Yoda, K., Hozumi, K. and Kira, T. (1964a) A quantitative analysis of plant form−the pipe model theory I. Basic analyses. Jpn. J. Ecol. **14**: 97-105

Shinozaki, K., Yoda, K., Hozumi, K. and Kira, T. (1964b) A quantitative analysis of plant form−the pipe model theory II. Further evidence of the theory and its application in forest ecology. Jpn. J. Ecol. **14**: 133-139

Sinoquet, H. and Rivet, P. (1997) Measurement and visualization of the architecture of an adult tree based on a three-dimensional digital device. Trees **11**: 205-210

Sinoquet, H., Le Roux, X., Adam, B., Ameglio, T. and Daudet, F. A. (2001) RATP: a model for simulating the spatial distribution of radiation absorption, transpiration and photosynthesis within canopies: application to an isolated tree crown. Plant Cell Environ. **24**: 395-406

Sumida, A., Nakai, T., Yamada, M., Ono, K., Uemura, S. and Hara, T. (2009) Ground-based estimation of leaf area index and vertical distribution of leaf area density in a Betula ermanii forest. Silva Fenn. **43**:799-816

Takeda, T., Oguma, H., Sano, T., Yone, Y. and Fujinuma, Y. (2008) Estimating the plant area density of a Japanese larch (*Larix kaempferi* Sarg.) plantation using a ground-based laser scanner. Agric. For. Meteorol. **148**: 428-438

Turner, D. P., Acker, S. A., Means, J. E. and Garman, S. L. (2000) Assessing alternative allometric algorithms for estimating leaf area of Douglas-fir trees and stands. For. Ecol. Manage.

126: 61-76

Van der Zande, D., Hoet, W., Jonckheere, L., van Aardt, J. and Coppin, P. (2006) Influence of measurement set-up of ground-based LiDAR for derivation of tree structure. Agric. For. Meteorol. **141**: 147-160

Wang, Y. P. and Jarvis, P. G. (1990) Description and validation of an array model−MAESTRO. Agric. For. Meteorol. **51**: 257-280

Warren Wilson, J. (1959) Analysis of the spatial distribution of foliage by two dimensional point quadrates. New Phytol. **58**: 92-101

Yamamoto, K. (2003) LIA32. http://www.agr.nagoya-u.ac.jp/~shinkan/LIA32/index-e.html (Accessed on 8 August 2015)

Zhu, J., Matsuzaki, T. and Gonda, Y. (2001) Wind profiles in a coastal forest of Japanese black pine (*Pinus thunbergii* Parl.) with different thinning intensities. Jpn. J. Ecol. **6**: 287-296

(Received 25 August 2015)

(Accepted 5 November 2015)

Appendix Abbreviations used in the text

Abbreviation	Explanation
b	Scaling exponent of a power trend line
c	Coefficient of a power trend line
G	Projected area of a unit foliage area
GLM	Generalized linear model
GLMM	Generalized linear mixed-effects model
G_t	Projection coefficient of twigs
H_t	Tree height (m)
H_l	Lowest foliage height (m)
IF	Intercept frequency of laser beams (m^{-1})
LAI	Leaf area index (m^2 m^{-2})
LAD	Leaf area density (m^2 m^{-3})
LA_s	Leaf area attached to a shoot (m^2)
l	Length of trace of a blocked laser beam in a voxel (m)
LiDAR	Light Detection And Ranging
N_i	Number of beams intercepted by obstacles in a voxel
PAD	Plant area density (m^2 m^{-3})
PAD_v	Plant area density in a voxel (m^2 m^{-3})
RMSE	Root−mean−square error
SIL	Sum of internode length (m)
SIL_s	Sum of internode length in a shoot (m)
SIL_v	Sum of internode length per unit volume in a voxel (m m^{-3})
TLS	Terrestrial LiDAR scanner
α	Mean length of a segment transecting a cross section of the beam Per unit area of cross section (m m^{-2})
θ	Laser incident zenith angle (rad)

Article

Classifying Managed and Unmanaged Bamboo Forests using Airborne LiDAR Data

Keiko Nagashima[*1], Yukihiko Kinami[*2*3] and Kazuhiro Tanaka[*1]

ABSTRACT

The goal of our study was to separate managed and unmanaged bamboo (*Phyllostachys pubescens*) forests based on the height and density of bamboo stems using LiDAR data. Based on 95% confidence intervals of the height of managed and unmanaged bamboo obtained during field surveys, stem height was classified as either "managed stem zone," "transitional zone," or "unmanaged stem zone." Using the digital canopy height model (DCHM, mesh size = 1.0 m) obtained from the LiDAR data for these three zones, bamboo forests successfully classified to "managed forests", "extensively managed forests" and "unmanaged forests". Density analysis was conducted using the marker-controlled watershed segmentation algorithm utilizing treetops obtained using the local maxima detection method (LM) with a circular window with a 1.0-m radius. Stem number obtained through LiDAR was compared to that obtained during field surveys by calculating the extraction rate. Stem numbers were underestimated in every management status category; with an increase in stem density, crown size decreased, which eventually lead to a low extraction rate. Because the estimated crown size of managed and unmanaged stems were approximately 1.0 m and 0.8 m, respectively, the DCHM with mesh size ≤ 0.5 m and a circular window size for LM with <1.0 m radius are required to classify the bamboo forest based on their management status.

keyword: bamboo, LiDAR, management status, stem height, stem density

INTRODUCTION

Abandonment and subsequent expansion of bamboo (*Phyllostachys pubescens*) forests has been widely observed in western Japan (Someya et al., 2010). The invasion and replacement of the surrounding forests by bamboo could result in a decline in biodiversity (Suzuki, 2010) and a reduction in the soil and water conservation capacity of the forest (Hiura et al., 2004; Torii, 2007). Therefore, bamboo range expansion has been investigated using aerial photographs (Torii and Isagi 1997; Nishikawa et al., 2005; Hayashi and Yamada, 2008) and satellite images (Koizumi et al., 2003; Ohno et al., 2004). However, few studies have focused on the remote classification of bamboo forests that are managed for shoot production versus abandoned, unmanaged forests. This information is necessary for the success of efforts to determine methods to cope with the bamboo expansion problem.

Recent progress in laser technology has enhanced our ability to quickly document the detailed forest structure with great accuracy. Airborne LiDAR data have been utilized to estimate stand level attributes, such as average tree height, individual tree crowns, tree density, and tree volumes (Hirata, 2005a,b; Kato et al., 2014). However, most studies have been conducted in coniferous or deciduous forests (e.g., Popescu et al., 2003; Hirata 2005a,b; Ito et al., 2009); whereas few have been conducted in bamboo forests (Miyasaka et al., 2009).

In this study, we classified managed and unmanaged bamboo forest using airborne LiDAR data. Our study area, Nagaokakyo City in Kyoto Prefecture (Fig. 1), is an important region for bamboo shoot ("*Kyo-takenoko*") production. Bamboo forests in this area are primarily managed for commercial bamboo shoot production, except for a few forests managed for personal use. Managed bamboo forests are controlled in such a way as to maintain low stem numbers (1,000−2,500 stems per hectare) (Shibata, 2003), whereas the stem numbers in unmanaged forest may reach 10,000−12,000 stems per hectare (Shibata, 2010). In addition, the tops of bamboo stems

Corresponding author: Keiko Nagashima
(nagakei@kpu.ac.jp)

[*1] Graduate School of Life and Environmental Science, Kyoto Prefectural University, 606-8522, 1-5 Shimogamo Hangi-cho, Sakyo-ku, Kyoto city.
[*2] Faculty of Life and Environmental Science, Kyoto Prefectural University, 606-8522, 1-5 Shimogamo Hangi-cho, Sakyo-ku, Kyoto city.
[*3] PASCO Corporation, 153-0043, 1-1-12 Higashiyama Meguro-ku, Tokyo

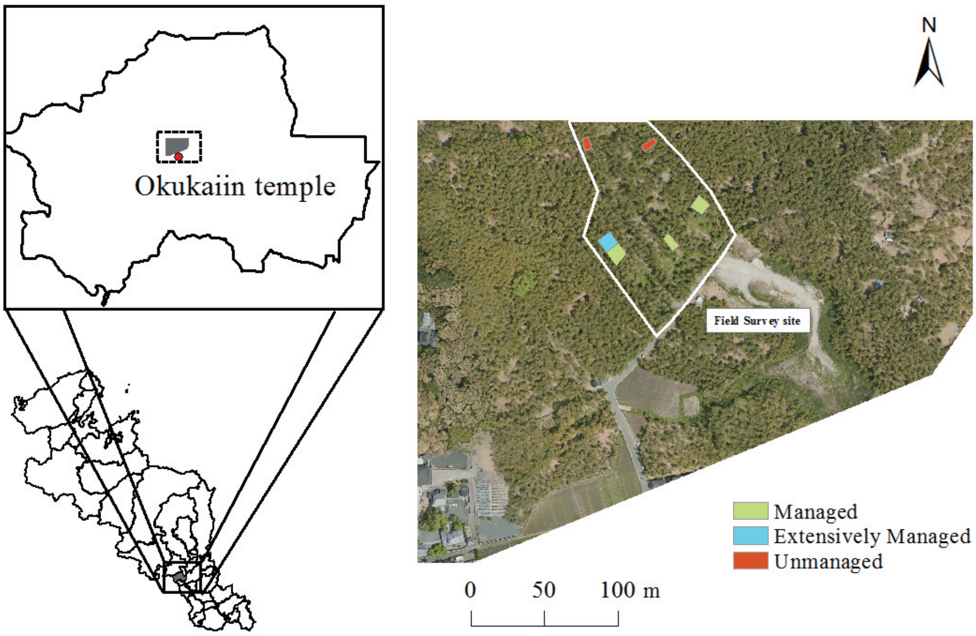

Fig. 1 Study area and sites for filed survey.

are broken off ("*Shindome*" in Japanese) when the number of nodes reach approximately 16 or 17 during May. This is done to reduce branch numbers and to prevent bamboo plants from being blown down by strong winds. It also reduces the amount of nutrients consumed for bamboo height, and thus, conserves nutrients for the growth of the shoot (Education Board of Nagaokakyo City, 2000). Therefore, the height of bamboo stems in managed forests is lower than that of unmanaged forests. Because airborne LiDAR data is known for its usefulness in providing both density and height of trees, we sought a method to separate managed and unmanaged bamboo forests based on the density and height of bamboo stems using LiDAR data.

MATERIALS AND METHODS

Study Area

Our study area comprised a bamboo forest around the Okukaiin temple located in the Nishiyama region of Nagaokakyo City, Kyoto Prefecture (Fig. 1). The total area of the bamboo forest was approximately 7.0 ha. The Nishiyama region has a hilly terrain with well-drained acidic soil, which is essential for bamboo shoot production. The climate of the regions is temperate, with an average temperature of 15℃ and total annual rainfall of 1,500 mm. Moderate rainfall from April to May occurs during the digging season of bamboo and from August to September when rhizomes grow. These conditions are favorable for bamboo shoot production (Education Board of Nagaokakyo City, 2000). Bamboo shoots have been produced historically in this region since the Edo era (in the 1800s). However, bamboo forests started to be abandoned when the import of cheap bamboo shoot increased in the Japanese market in the 1980s. Consequently, as observed in other places in Japan, the expansion of bamboo forests to higher elevations in mountainous areas has been reported (Torii and Isagi, 1997). However, a few managed forests for bamboo shoot production still exist, and therefore, managed and unmanaged forests co-exist in the region. In addition, there are some extensively managed forest areas that are managed mainly for personal use, and thus, the density and height of the bamboo stems are not strictly controlled. The study area around the Okukaiin temple is similar to other areas of bamboo forests in Nagaokakyo City. Managed bamboo forests are distributed in the gentle hills of the southern part of the area and unmanaged forests have gradually moved to the steeper northern slopes.

LiDAR and GIS data

LiDAR data utilized during this study, which belongs to Suntory Holdings Ltd. and Nishiyama Forest Management Promotion Committee, consisted of a 1 m mesh digital surface model (DSM) and digital terrain model (DTM) acquired on May 14, 2011 using a helicopter equipped with the SAKURA II sensor system of Nakanihon Air Services (Table 1). The DSM and DTM were generated by Nakanihon Air Services and provided to us through Nagaokakyo City. The bamboo forest distribution map was developed by modifying the 6th vegetation map of the National Environmental Information GIS (Biodiversity Center of Japan, 2004) based on the

Table 1 Performance characteristics of the LiDAR system

Senser	LMS-Q560
Flight altitude	300m
Flight speed	100km/h
Beam divergence	0.5 mrad
Laser pulse frequency	100,000 Hz
Scan width	±30°
Average distance between footprints	
along the scan line	0.35m
along the flight line	0.38m

*manufactured by RIEGL Laser Measurement Systems GmbH orthonized aerial photograph taken on May 14, 2011 together with the LiDAR data.

Field data collection

Field investigations were conducted during September 2011 in the bamboo forest in our study area (Fig. 1). The forest was owned by the same individual and consisted of bamboo forests that were managed, extensively managed, and unmanaged. We established two 10 m × 10 m and one 5 m × 10 m plots in managed forest, one 10 m × 10 m plot in the extensively managed forest, and two 5 m × 10 m plots in the unmanaged forest. Flat slopes rather than ridges or valleys were selected, and gaps were avoided in the selection of the study plots; these factors resulted in size differences of the plots. No clear boundary existed between managed and extensively managed stands. Therefore, the extensively managed plot was established at a place with a relatively large number of bamboo stems compared to the managed stand. At each plot, bamboo stem numbers were counted to determine stem density. A total of 23 top broken bamboo stems (managed stems) and 34 unbroken stems (unmanaged stems) were detected in the plots and the heights of the stems were measured. We measured stem height as the height from the base, in contact with the ground, to the highest position of the standing bamboo stem (i.e., the height expected based on the LiDAR). Therefore, this measurement was different from stem length. The coordinates for the corners of each plot were determined with a handheld GPS (Garmin GPSmap 64s) and the data were imported into the GIS to establish polygons for each plot.

Data analysis

The digital canopy height model (DCHM) was computed by subtracting the DTM from the DSM. The DCHM of the bamboo forest was determined by masking a bamboo forest distribution map. Grid cells <4 m that consisted of gaps in the bamboo forest were excluded from the DCHM, and these data were utilized for analyses. Two methods, stem height-based and density-based, were adopted to classify managed, extensively managed, and unmanaged bamboo forests. The analytical process for each method is given below.

Height-based analysis

The average height of managed and unmanaged stems was calculated based on height data for 23 managed stems and 34 unmanaged stems. We determined significant differences in the height of managed and unmanaged stems using a *t*-test. We calculated a 95% confidence interval for height of both managed and unmanaged stems. Based on the confidence intervals, the height of stems was classified into three groups: a "managed stem zone" with the maximum height of the upper limit of the confidence interval for the managed stems, a "transitional zone," in which height was greater than the upper limit of the confidence interval for managed stems, but lower than the lower limit of the confidence interval for unmanaged stems, and the "unmanaged stem zone" which height was greater than the lower limit of the confidence interval for unmanaged stems. Utilizing these three classes for displaying the DCHM, we hypothesized that managed forest plots would primarily consist of grid cells in the "managed stem zone," unmanaged forest plots would mainly consist of grid cells in the "unmanaged stem zone," and extensively managed forest plots would be a mixture of grid cells in the "transitional zone" and "unmanaged stem zone." In other words, managed or unmanaged bamboo forests might show a homogeneous structure consisting of grid cells in the "managed stem zone" or "unmanaged stem zone." The extensively managed forest might comprise a mosaic of grid cells in the "transitional zone" and "unmanaged stem zone." Although each grid cell of the LiDAR data does not always indicate the height of the bamboo top, we considered that management type might be discernable if we looked at the "zone structure" consisting of the bamboo forest.

Density-based analysis

Detecting and delineating individual trees is essential for calculating the density of bamboo stems. Methods developed for optical imagery, such as the valley following, watershed segmentation, and local maxima detection method (LM) have been extended to LiDAR data (Chen et al., 2006; Kwak et al., 2007); however, a tendency for overestimation has been observed (Kwak et al., 2007). To avoid this problem, flexible window sizes based on the tree height and crown size were incorporated into the LM (Popescu and Wynne, 2004) for detecting treetops. Variable window size was also applied to identify the treetops and conduct watershed segmentation around them, which is called marker-controlled watershed segmentation (Chen et al., 2006). Previous studies have revealed window size strongly related to crown size. Based on the mesh size of the DCHM (1.0 m) and the 1.2 m average radius of bamboo tree crown size indicated by Katanoda (2004), we applied the LM on the DCHM by using the Focal Statistics tool in ArcGIS with a circular window with a 1.0-m radius, which is the smallest available window size. By using the treetops obtained by the LM as a marker, marker-controlled watershed segmentation was implemented using the Watershed tool of ArcGIS Spatial Analyst. To determine the boundary between crowns, a sharpening (high-pass) filter was applied to the DCHM of bamboo forests before detecting the treetops.

The result of marked-controlled watershed segmentation was then clipped by the polygons for each plot. The number of tree crowns whose treetops were included in the plot were counted and compared with the stem number obtained during the field surveys based on the extraction rate (extraction rate = (N_{Test}/N_{Ref}), where N_{Test} is the number of trees detected by the marker-controlled watershed algorithm and N_{Ref} is the number of trees observed during the field surveys). Stem density (stems per 100 m^2) of each plot and the mean density by management status were also calculated based on the field survey data. In order to estimate the crown size, the radius of the area that could be occupied by one stem at each plot was calculated by dividing the plot area by stem number observed in the field survey. The mean estimated crown size for each management status was also calculated. Relationships between stem density and extraction rate, and between stem density and estimated crown size were investigated by fitting logarithmic trend-lines to determine the accuracy of the stem density-based method.

The Karnel density tool of ArcGIS Spatial Analyst was utilized to calculate and display the stem density of bamboo forests based on the treetop data obtained by the LM. The value of cell size was set to default for the output raster and the search radius for calculation. Lower densities were expected in managed forest plots and higher densities were expected in unmanaged forest plots.

RESULTS

Height-based analysis

Average heights of managed and unmanaged stems were 9.7m and 14.8 m, respectively, and the height of managed stems was significantly smaller than that of unmanaged stems (t-test, $p < 0.001$, Fig. 2). The 95% confidence interval of managed stems was from 8.8 m to 10.6 m, whereas that of unmanaged stem was from 13.8 m to 15.6 m. As a result, we classified bamboo up to 10.6 m as being in the "managed stem zone," bamboo taller than 10.6 m and shorter than 13.8 m as in the "transitional zone," and bamboo taller than 13.8 m as belonging to the "unmanaged stem zone." Displaying the DCHM by those three zones (Fig. 3), clear trends were observed. Managed plots were in a mixture of the "managed stem zone" and "transitional zone." Extensively managed plots were consisted with grid cells in the "transitional zone" and "unmanaged stem zone." Unmanaged

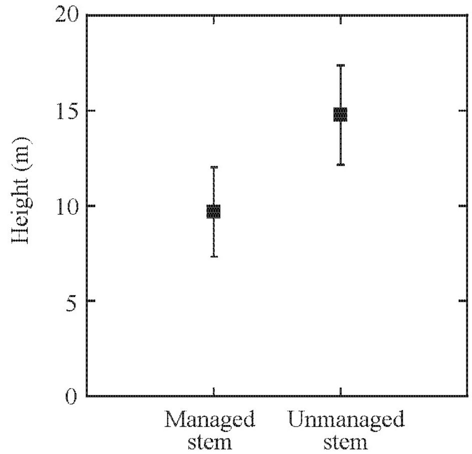

Fig. 2 Height of managed and unmanaged stems obtained by the field survey.

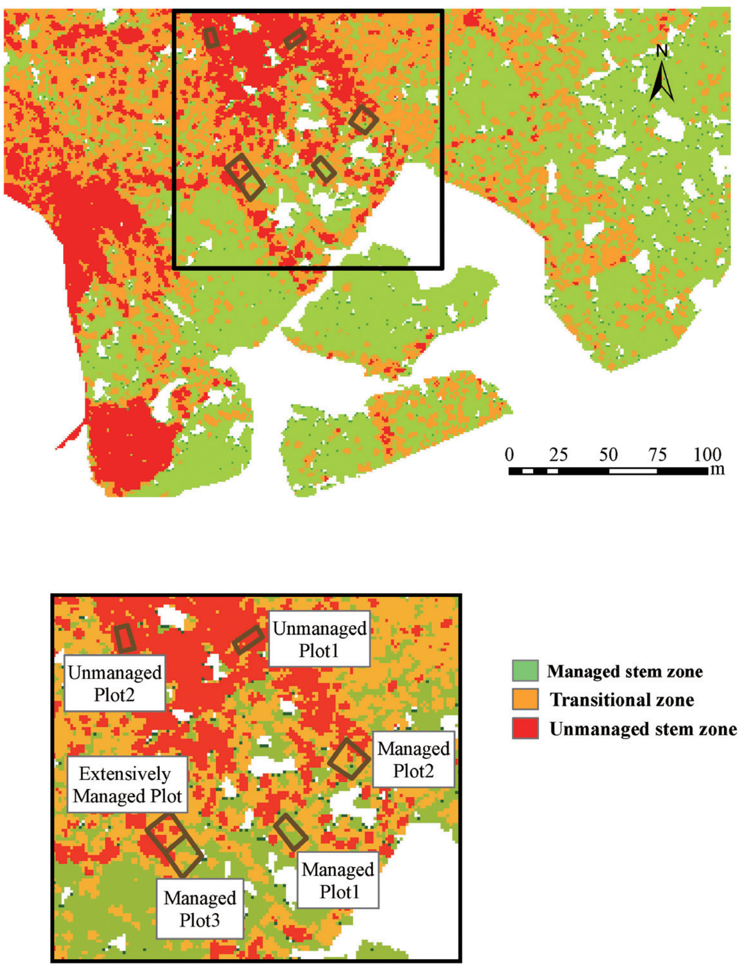

Fig. 3 Classification of DCHM by the three zones of "managed stem zone", "transitional zone" and "unmanaged stem zone".

plots were mainly consisted with grid cells in the "unmanaged stem zone."

Density-based analysis

The average stem density of the managed plots, extensively managed plot, and unmanaged plots were 22.33 stems/100 m^2, 30 stems/100 m^2, and 50 stems/100 m^2, respectively (Table 2). Our data indicated an increase in stem density as management activities declined. Using the marker-controlled watershed segmentation algorithm, the mean extraction rate decreased as the management activities declined: the mean extraction rates of managed, extensively managed, and unmanaged plots were 68.06%, 46.67%, and 22.56%, respectively (Table 2). However, comparing the extraction rate by plots, large differences were observed between managed plot 1 (38.46%) and plot 2 (85.71%) or plot 3 (80.00%). Although the differences were small, these differences among plots in managed areas were also found in the stem density and estimated radius of crown size: stem density was greater (26 stems/100 m^2) and the estimated crown size was smaller (1.10 m) in plot 1 than in the other two plots (Table 2). In terms of the relationship of extraction rate and stem density by plots, the extraction rate decreased along with the increase in stem density (logarithmic trend-line; R^2 = 0.9205, Fig. 4a). The estimated crown size also decreased as the stem density increased (logarithmic trend-line; R^2 = 0.9953, Fig. 4b)

Based on the stem density of bamboo forests using the Karnel density tool, two of the three managed plots (plots 2 and 3) were in the category from 1000 to 2100 stems per hectare, but the extensively managed and unmanaged plots showed lower densities of 1000−1500 stems per hectare (Fig. 5). No area higher than 2100 stem per hectare was obtained by the calculation.

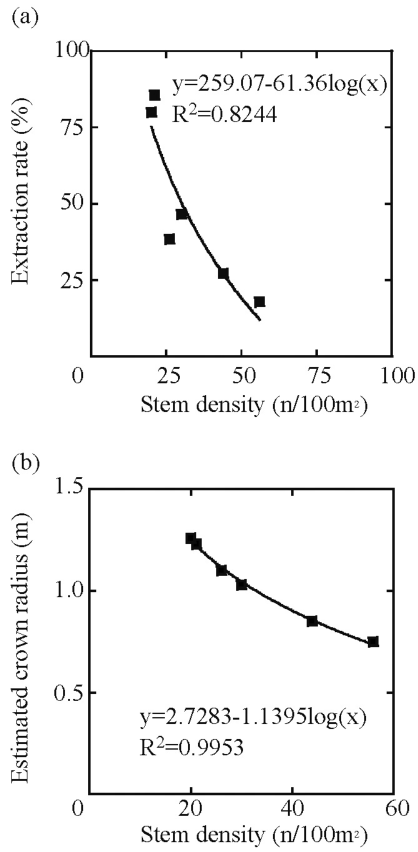

Fig. 4 Relationship between stem density and extraction rate (a) and between stem density and estimated crown radius(b).

DISCUSSION

The results of the stem height-based analysis showed different tendencies among different management status categories. Managed plots, in which stems tended to be shorter because the tops were broken off, consisted with grid cells in the "managed stem zone" and "transitional zone." Unmanaged plots, in which stems tended to be taller because tops were not broken, show a homogeneous structure consisting of grid cells in the "unmanaged stem zone." Because height control of the bamboo stems was not always conducted, the extensively managed plots consisted with grid cells in "transitional zone" and "unmanaged stem zone." These findings were similar to the expected, which suggests the utility of the stem height-based analysis to determine management status of bamboo forests. Similarly, the height of conifer trees was well predicted using LiDAR data with r^2

Table 2 Bamboo stems number by marker−controlled watershed segmentation and field survey

Management status	Plot no.	plot size (m^2)	Stem numbers: Marker−controlled watershed segmentation	Stem numbers: Field survey	Extraction rate (%)	Mean extraction rate (%)	Stem density (n/100m^2)	Mean stem density (n/100m^2)	Estimated crown radius (m)	Mean estimated crown radius (m)
Managed	plot1	50	5	13	38.46	68.06	26	22.33	1.10	1.20
	plot2	100	18	21	85.71		21		1.23	
	plot3	100	16	20	80.00		20		1.26	
Extensively managed	−	100	14	30	46.67	46.67	30	30.00	1.03	1.03
Unmanaged	plot1	50	6	22	27.27	22.56	44	50.00	0.85	0.80
	plot2	50	5	28	17.86		56		0.75	

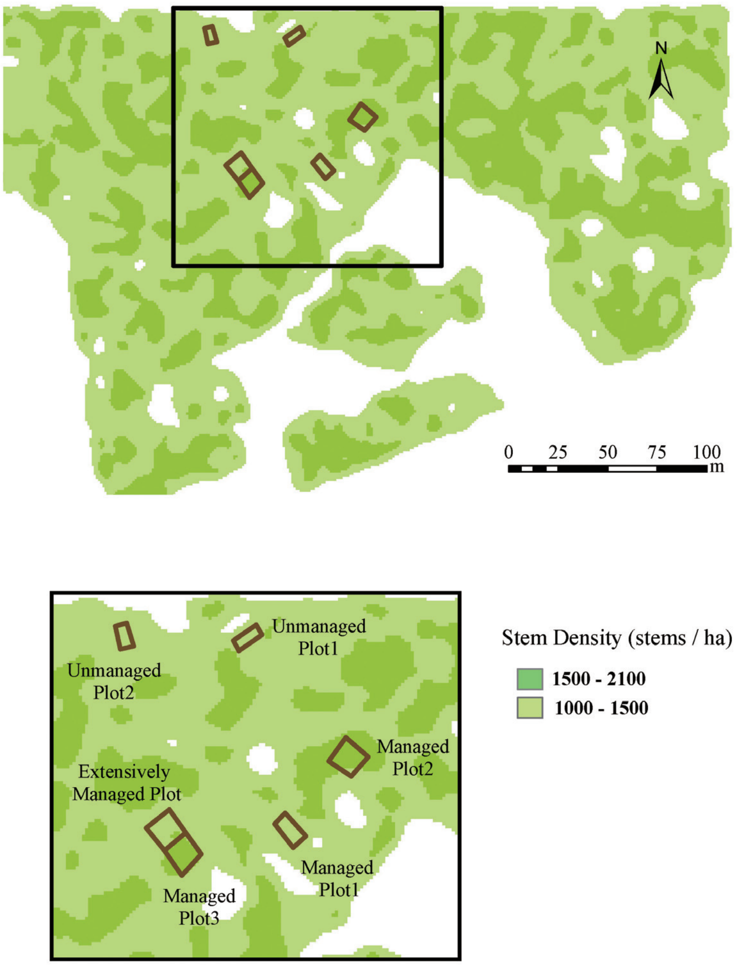

Fig. 5 Stem density of the bamboo forests calculating by the Karnel Density tool of ArcGIS.

values of approximately 0.9 (Naesset, 1997; Means et al., 2000; Takahashi et al. 2005), although a slight tendency for underestimation was observed (Taguchi et al., 2008; Gaveau and Hill 2003). Although we did not investigate the accuracy of height because it was difficult to recognize the sample stem and obtain its height from the DCHM, our results indicate the high possibility of LiDAR data utilization for estimating the height of bamboo stems.

Although the mean extraction rate of managed plots was relatively high (68.06%) compared to extensively managed and unmanaged plots, the detected stem numbers by LiDAR data were all underestimated (Table 2). In addition, the mean extraction rate exhibited a decreasing trend as management activities declined. Conversely, stem density exhibited an increasing trend as the management status declined. The same trend was also found among the managed plots; the extraction rate of plot 1, which had a greater stem, was lower than the other two plots. These results show that stem density is the factor with the best extraction rate; this was also confirmed by the decreasing tendency of extraction rate with the increase in stem density (Fig. 4a). In addition, stem density was also related to crown size, with stem density exhibiting a negative relationship with crown size (Fig. 4b, Table 2). Those results indicated that as the stem density increases, crown size becomes smaller, which leads to a low extraction rate. The low extraction rate in higher density areas directly reflected the results of our calculations displayed by the stem density of bamboo forests using the Karnel density tool. The stem density calculated for managed plots 2 and 3, showed a relatively high extraction rate of 1,500 to 2,100 stems per hectare, almost identical to what was calculated at plot level (Table 2). However, the stem density of plot 1, the smaller of the managed plots, and extensively managed and unmanaged plots was calculated as 1,000 to 1500 stems per hectare, which much lower than the real stem density of 2,600 to 5,600 stems per hectare.

Successful identification of individual trees depends on the filter window size for the LM methods together with the mesh size of the DCHM data. Errors of commission or omission could occur if the filter window size for LM is too small or too large, and it is strongly related to the crown size (Wulder et al., 2000). In addition, the mesh size of the DCHM also reflected the accuracy of individual tree detection and it was strongly related to crown size (Hirata, 2005). Although the estimated crown sizes for managed and extensively managed plots were around 1.0 m, the smaller crown size in unmanaged plots (mean value = 0.80 m) suggested utilizing a smaller window size for detecting treetops. The filter size we utilized was the minimum size applicable to our 1.0 m DCHM data. Smaller filter size, therefore requires a smaller mesh size for the DCHM data. Popescu et al. (2003) accomplished individual tree detection for coniferous and deciduous trees using the LM by changing the variable window size according to the relationship between tree height and crown size. The window size in the study varied between 3 × 3 and 31 × 31 pixels, which corresponded to crown sizes of 1.5 m to 15.5 m, respectively, when the mesh size was 0.5 m. Together with our results, this suggests that the DCHM with mesh size ≤ 0.5 m and a circular window with <1.0 m radius are required to classify bamboo forest based on their management status.

The management regime of bamboo forest might be another reason for the low extraction rate of managed plot 1. In managed bamboo forests, the top of the bamboo stem is broken off. This makes the top of the crown flat, which resulted in small height differences with the adjacent bamboo stems. Thus, as a larger number of top broken stems exist, treetop detection by the LM might become more difficult. Because we did not have data on the number of top broken stems, additional research is required to assess this hypothesis.

CONCLUSIONS

Our goal was to explore ways to divide managed and unmanaged bamboo forests based on the height and the density of bamboo stems. The stem height-based analysis classified the three forest types within different management status categories. The managed forest consisted with grid cells in the "managed stem zone" and "transitional zone," extensively managed forests consisted with grid cells in the "transitional zone" and "unmanaged stem zone," and unmanaged forests show a homogeneous structure consisting of grid cells in the "unmanaged stem zone." Thus, stem height-based analysis might be a useful method for classifying managed and unmanaged bamboo forests. However, this method is only useful when the tops of bamboo stems are broken off as a management regime for producing bamboo shoots. In other words, it is only useful for the area where "*Shindome*" is conducted.

Stem density-based analysis, on the other hand, is a useful method applicable worldwide. However, stem numbers tended to be underestimated in every management status category because of the larger mesh size of the DCHM and the window size compared to the estimated crown size, especially for the unmanaged forest. Utilization of smaller mesh and smaller window sizes might improve the accuracy of this analysis. The possibility that breaking bamboo tops affects the extraction rate of individual stems should be further investigated.

ACLKNOWLEDGEMENT

We would like to express our appreciation to Nagaokakyo City, Suntory Holdings Ltd. and Nishiyama Forest Management Promotion Committee for providing the LiDAR data for the study area.

LITERATURE CITED

Biodiversity Center of Japan (2004) The 6th vegetation map of Natural environmental information GIS, http://www.biodic.go.jp/trialSystem/top.html (Accessed on 1st July, 2014)

Chen, Q., Baldocchi, D., Gong, P., Kelly, M. (2006) Isolating individual trees in a Savanna woodland using small footprint Lidar data. Photogram. Eng. Rem. Sens. **72**: 923-932

Education Board of Nagaoka city (2000) Kyo-takenoko to kajibunka [Kyo-takenoko and smith culture] (in Japanese). Education board of Nagaoka city, Kyoto, 247pp

Gavaeau, D. L. A., Hill R. A. (2003) Quantifying canopy height underestimation by lase pulse penetration in small-footprint airborne laser scanning data. Can. J. Remote Sens. **29**: 650-657

Hayashi, K., Yamada, T. (2008) Is bamboo stand expansion independent of topographic conditions? Jpn. J. Conserv. Ecol. **13**: 55-64

Hirata, Y., (2005a) Influence of transmittance and sampling density of laser beams in forest measurement of a *Cryptomeria japonica* stand with an airborne laser scanner. Jpn. J. For. Plann. **39**: 81-95

Hirata, Y. (2005b) Forest measurement of *Cryptomeria japonica* stand and *Chamaecyparis obtuse* stand with an airborne laser scanner. J. Jpn. Soc. Photo. Remote Sens. **44** (6): 14-17 (in Japanese)

Hiura, H., Arikawa, T., Bahadur, D. D. (2004) Risks of sediment related disasters due to the abandoned expanding bamboo stands at the foot of slopes surrounding city area. J. Jpn. Landslide Soc. **41**: 323-334

Itoh T., Matuse, K., Naito, K. (2009) Reproducibility of tree crown using airborne LiDAR. J. Jpn. For. Soc. **91**: 326-334

Katanoda, I. (2004) Relationship between hinoki crowns and foliage of *Phyllostachys pubescens* invaded hinoki plantation. Kyushu J. For. Res. **57**: 99-103

Kato, A., Ishii, H., Enoki, T., Osawa, A., Kobayashi, T., Umeki, K., Sasaki, T., Matsue, K. (2014) Application of laser remote sensing to forest ecological research. J. Jpn. For. Soc. **96**: 168-181

Koizumi, K., Tanimoto, C., Piao, C. (2003) Extraction of bamboo stands by observing Landsat 5-TM. J. Jpn. Soc. Photo. Remote Sens. **42** (6): 42-51 (in Japanese)

Kwak, D., Lee, W., Lee, J., Biging, G.S., Gong, P. (2007) Detecting of individual trees and estimation of tree height using LiDAR data. J. For. Res. **12**: 425-434

Means, J. E., Acker, S. A., Fitt, B. J., Renslow, M., Emerson, L., Hendrix, C. J. (2000) Predicting forest stands characteristics with airborne scanning lidar. Photogram. Eng. Rem. Sens. **66**: 1367-1371

Miyasaka, S., Yada, Y., Niba, T., Yoshida, N., Unome, S., Nakamura, K. (2009) Airborne remote sensing survey for bamboo distribution in satoyama area of Kanazawa city. J. Remote Sens. Soc. Jpn. **29**: 586-591

Nishikawa, R., Murakami, T., Yoshida, K., Mitsuda, Y., Nagashima, K., Mizoue, T. (2005) Characteristic of Temporal range shifts of bamboo stands according to adjacent landcover type. J. Jpn. For. Soc. **87**: 402-409

Næsset, E. (1997) Estimating timber volume of forest stands using airborne laser scanner data. Remote Sens. Environ. **61**: 246-253

Ohono, T., Shimomura, Y., Maenaka, H., Masuda, N. (2004) Study on the traditional and the prediction of the expansion of bamboo forests. Landscape. Res. J. **67**: 567-572

Popescu, S. C., Wynne, R. H., Nelson, R. F. (2003) Measuring individual tree crown diameter with lidar and assessing its influence on estimating forest volume and biomass. Can. J. Remote Sens. **29**: 564-577

Popescu, S., Wynne, R.H. (2004) Seeing the trees in the forest: using Lidar and multispectral data fusion with local filtering and variable window size for estimating tree height. Photogram. Eng. Rem. Sens. **70**: 589-604

Shibata, S. (2003) *Phyllostachys pubescens* and Japanese. J. Jpn. Soc. Revegt. Tech. **28**: 406-411

Shibata, S. (2010) Bamboo forest management toward effective utilization of bamboo resources. Shinrinkagaku **58**: 15-19

Someya, T., Takemura, S., Miyamoto, S. Kamata, M. (2010) Predictions of bamboo forest distribution and associated environmental factors using natural environmental information GIS and digital national land information in Japan. Landscape Ecol. Manag. **15**: 41-54

Suzuki, S. (2010) Are bamboo forests low in vegetation diversity? Shinrinkagaku **58**: 11-14

Taguchi, H., Endo, T., Yasuoka, Y. (2008) Detection of model-based individual conifer tree crown and estimation of tree height using LiDAR point clouds. J. Remote. Sens. Society Jap. **28**: 331-341

Takahashi, T., Yamamoto, K., Senda, Y., Tsuzuku, M. (2005) Estimating individual tree heights of sugi (*Cryptomeria japonica* D. Don) plantations in mountainous areas using small-footpring airborne LiDAR. J. For. Res. **10**: 135-142

Torii., A., Isagi, Y. (1997) Range expansion of bamboo species in southern areas of Kyoto Prefecture, Japan. Jpn. J. Eco. **47**: 31-41

Wulder, M., Niemann, K. O., Goodenough, D. G. (2000) Local maximum filtering for the extraction of tree locations and basal area from high spatial resolution imagery. Remote Sens. Environ. **73**: 103-114.

(Received 22 July 2015)
(Accepted 14 November 2015)

GUIDE FOR CONTRIBUTORS

Please refer to the following guidelines when submitting a new manuscript to the JOURNAL OF FOREST PLANNING ("the *Journal*"), of the Japan Society of Forest Planning ("the *Society*"), so that your manuscript may be handled expeditiously.

Type of Papers: Each paper is classified into one of three types: article, review, or short communication. A paper should be a report of original research that has not been submitted elsewhere (other than as an abstract).

Contributors: The first author of a paper of any type should be a member of the *Society* unless he/she is invited by Chief Editor. The authors can apply for membership on submission.

Copyright: The *Society* reserves all right to the papers for the Journal. Written permission by the Chief Editor is required for reproduction or republication.

Decision for Publication: The Editorial Board makes the decision to accept, reject, or suggest corrections of a manuscript in accordance with the results of reviews by knowledgeable referees selected by the Editorial Board.

Manuscript: Manuscript should be written in English in line with the guideline in "Manuscript Preparation" below.

English: All authors whose first language is ***not*** English should ask a native speaker to refine the written English before submission.

Final Manuscript and Authors' Corrections: When the manuscript is accepted, the authors will be asked to send the final manuscript in electronic forms. The required formats will be indicated in the manuscript preparation. The author's proof will be sent only once for misprint corrections.

Expense on Publication: Printing costs will be free. A free electronic reprint will be sent to the author in Portable Document Format (pdf). Authors who require the color page/special printing should pay the actual expense (¥20,000/page). Printed offprint can also be ordered with the cost of ¥6,000 per printed pages (50 copies).
(All prices are subject to change.)

Submission and Inquiry: The manuscript and a submission form should be sent in electronic format to the chief editor in Portable Document Format (pdf) by email. The chief editor's email address can be found on the inside cover of the journal. Inquires about submission may also be sent to the chief editor by email.

(revised August, 2015)
(revised April, 2013)

MANUSCRIPTS PREPARATION

Style: A manuscript should be arranged as follows: (1) Title of paper, authors' full names and affiliations with addresses, (2) Abstract, (3) Keywords (no more than five), (4) Main text, (5) Literature cited, (6) Figures and tables, (7) Messages to Editors.

Typing: Manuscripts should be typewritten, double-spaced on one side of A4 white paper with margins of 3 cm on top, bottom and both sides. The desired location of tables and figures should be indicated in the text with red ink in the right margins.

Text Style: Characters to be printed in *italic* or **bold** should be entered using the features of the word processing software.

Abstract: An abstract is required for any type of papers, and should be no more than 500 words.

Literature Cited: Literature cited should be listed alphabetically by first author's surname (family name). For the style, consult the examples given below. Literature in the text may be cited by author's surname and year of publication in parentheses after the statement concerned. If there are more than two authors, citations should quote the surname of the first author and the words "et al.". All authors' names should be included in the list.

a. For periodicals: Yamamoto, N. and Sasaki, S. (1976) Electron microscope study on polysome formation during pine seed germination. J. Jpn. For. Soc. **58**: 65-66
b. For books: Levitt, J. (1972) Responses of plants to environmental stresses. Academic Press, New York & London, 697pp
c. For edited books: Gadow, K. V. (2005) Science-based forest design and analysis. In: Naito K. (eds) The role of forests for coming generations. Jpn. Soc. For. Plan. Press, Utsunomiya: 1-19
d. For Internet resources: McGaughey, R. J. (1999) Visualization System. USDA Forest Service, Pacific Northwest Research Station.

http://faculty.washington.edu/mcgoy/svs.html
(accessed on Apr. 14, 2013)

Tables: There must be numbered with Arabic numerals according to their sequence in the text (Table 1, Table 2 etc.). Each table should be prepared on a separate sheet. Each table should have a brief and self-explanatory title. Any explanation for tables should be given as a footnote at the bottom of the table.

Figures: Figures must be numbered with Arabic numerals according to their sequence in the text. Each figure should be prepared on a separate sheet. Each figure's legend should be prepared on another separate sheet. Figures should be of publication quality. Color figure can be included for an extra printing charge. A figure for color printing should be indicated by a note, "COLOR", on the margin of the sheet.

Submission Form: The submission form should be filled out and attached to the manuscript on submission. The form can be found at the last page of the *Journal*. Non-member authors can apply for memberships of the *Society* at the time of submitting their paper by enclosing the application form, which can be found on the inside of the back cover of the *Journal*.

Electronic submission: Authors are required to submit their manuscript in electronic format (pdf file) by email. If it is difficult to save the manuscript in pdf, MS-Word files are also accepted. Authors are encouraged to save tables and figures in pdf form and combine them with the manuscript file. This means that just one pdf file should be sent to the chief editor. After acceptance, the authors will be asked to submit the final manuscript in the following formats:

1) Abstract & Keywords: an MS Word (doc or docx) file
2) Main text & Literature cited: an MS Word (doc or docx) file
3) Figures: an MS PowerPoint (ppt or pptx) file or a PDF file or a high-quality image file (tiff, jpg or png)
4) Tables: an MS Excel (xls of xlsx) file or an MS PowerPoint (ppt or pptx) file

(May, 2001)
(revised September, 2002)
(revised February, 2009)
(revised April, 2013)
(revised August, 2015)

JOURNAL OF FOREST PLANNING

Submission Form

1. Date of submission: ____________________

2. Name of author(s): ____________________

____

3. Title of manuscript: ____________________

____

4. Corresponding author: ____________________

5. Affiliated institution: ____________________

6. Mailing address: ____________________

____

Telephone: ____________ Fax: ____________

E-mail: ____________________

Mailing address in Japanese (if available): ____________________
(確実に郵送できるように送付先を研究室名等までお書きください)

____

____

7. Classification of manuscript*: □article □review □short communication
*Plaese tick one of the boxes.

8. Number of pages including abstracts: ____________

9. Number of tables: ____________ Number of figures: ____________

10. Necessary number of reprints: ____________

11. Please tick either which apply:
□The written English has been proofread by a native speaker.
□I am from an English-speaking country.

Filled by the Editorial Board

受付番号 ____________

受付日 ____________ 受理日 ____________

Japan Society of Forest Planning